Int. J. Morphol.,
42(5):1361-1372, 2024.

Exploring the Anti-Cancer Properties of *Nasturtium officinale* L. via the HOTAIR/miR-124/Notch1 Pathway in Rat Hepatocellular Carcinoma: An Investigation Using Biochemical, Molecular, Immunohistochemical, and Histopathological Methods

Exploración de las Propiedades Anticancerígenas de *Nasturtium officinale* L. a Través de la vía HOTAIR/miR-124/Notch1 en el Carcinoma Hepatocelular de Rata: Una Investigación Utilizando Métodos Bioquímicos, Moleculares, Inmunohistoquímicos e Histopatológicos

Huichao Feng[1#]; Sheng Zheng[2#]; Juan Yang[2]; Xiaozhou Mao[3]; Tao Liu[3]; Qiuxin Zhang[3] & Yaqin Chen[4]

FENG, H.; ZHENG, S.; YANG, J.; MAO, X.; LIU, T.; ZHANG, Q. & CHEN, Y. Exploring the anti-cancer properties of *Nasturtium officinale* L. via the HOTAIR/miR-124/Notch1 pathway in rat hepatocellular carcinoma: An investigation using biochemical, molecular, immunohistochemical, and histopathological methods. *Int. J. Morphol., 42(5)*:1361-1372, 2024.

SUMMARY: This study aimed to explore the potential of *Nasturtium officinale* L. leaves extract (NOLE) in safeguarding hepatocytes against N-diethylnitrosamine (DEN)-induced hepatocellular carcinoma (HCC) by investigating its effects on biochemical, molecular, and antioxidant pathways. The study also delved into NOLE's role in modulating the HOTAIR/miR-124/Notch1 axis pathway. In this study, 50 Wistar rats were divided into five groups (n=10/group): normal, HCC-induced (100 mg/kg DEN), HCC rats treated with 100 and 200 mg/kg DEN + NOLE, and normal rats treated with 200 mg/kg NOLE. At the study's conclusion, serum levels of liver function markers (such as albumin, total protein, bilirubin, C-reactive protein, ALT, AST, and ALP), inflammatory cytokines (IL-6, IL-1b, IL-10, and TNF-a), and oxidative parameters [including glutathione peroxidase (GPx), superoxide dismutase (SOD), catalase (CAT) enzyme activity, and nitric oxide (NO) levels] were assessed. The levels of HOTAIR, miR-124, Notch1, and Jagged1 genes and proteins in liver tissue were measured. Immunohistochemical analysis was used to evaluate P53-positive cells in liver hepatocytes. DEN administration led to significant alterations in body and liver weight, serum liver enzymes, antioxidant levels, inflammatory markers, and expression of genes/proteins related to the HOTAIR/miR-124/Notch1 axis in liver pathways. NOLE exhibited dose-dependent effects in mitigating these changes, notably enhancing weight, liver health, antioxidant capacity, and inflammatory responses, especially at the 200 mg/kg dosage. Histopathological assessments revealed structural improvements in liver tissue with NOLE treatment. In conclusion, our study highlights the potential of NOLE in exerting anti-cancer effects against DEN-induced HCC.

KEY WORDS: *Nasturtium officinale* L.; N-diethylnitrosamine; HOTAIR; Liver; Hepatocellular carcinoma.

INTRODUCTION

Hepatocellular carcinoma (HCC) is the primary form of liver cancer, with an annual incidence ranging between 500,000 to 1,000,000 new cases and resulting in roughly 600,000 deaths each year. The highest rates occur in Asia (55 per 100,000), while Europe reports the lowest rates (5 per 100,000) (Singal *et al*., 2023). Genetic mutations, such as focal deletions affecting tumor suppressors (PTEN, p53, and CDKN2B) and focal amplifications affecting oncogenes (MET, MYC, and FGF19), along with alterations in signaling pathways (including Notch, PI3K/AKT/mTOR, p53/p21, HOTAIR/Notch1, Wnt/b-catenin, and JAK/STAT), significantly impact metabolic processes, cell cycle regulation, repair mechanisms, angiogenesis, and immune responses within hepatocytes and other liver parenchymal cells, ultimately leading to tumor formation (Garcia-Lezana *et al*., 2021). Primary risk factors associated with HCC

[1] Department of General practice, Shenzhen Pingshan District Central Hospital, Shenzhen Guangdong, 518122, China.
[2] Department of Gastroenterology, The Third People's Hospital Of Yunnan Province,Kunming Yunnan, 650011, China.
[3] Graduate School of Clinical Medicine Dali University, Dali Yunnan, 671000, China.
[4] Department of Pediatrics, The First Affiliated Hospital of Zhejiang Chinese Medical University, Zhejiang Hospital of Traditional Chinese Medicine, Hangzhou Zhejiang, 310006, China.
[#] Huichao Feng and Sheng Zheng are co-first authors, they contributed equally to this work.

Received: 2024-05-31 Accepted: 2024-06-17

include viral hepatitis (hepatitis B and C), exposure to toxins (such as aflatoxins, certain chemotherapy drugs, alcohol, and nitrate-based compounds), metabolic conditions (such as fatty liver disease, diabetes, and hereditary hemochromatosis), and immune-related disorders. Additionally, pro-inflammatory cytokines (such as IL-6, IL-1β, IL-10, and TNF-α), as well as reactive oxygen species (ROS) and reactive nitrogen species (RNS), play significant roles in creating a tumor-friendly microenvironment that supports the growth of liver tumors (Thylur *et al*., 2020).

Nitrosamines, also known as N-nitrosamines, are a group of organic carcinogenic compounds characterized by the chemical formula R2N-N=O. These substances are formed through the interaction of nitrous acid (HNO2) with secondary amines. Nitrosamines are commonly present in tobacco, vehicle exhaust, cosmetics, canned food products, and foods that undergo cooking or frying processes, such as meats, bread, and vegetables (Stanfill *et al*., 2023). Various types of nitrosamines, including N-diethylnitrosamine (DEN), N-Nitrosoanabasine, N-Nitrosodimethylamine, N-Nitrosonornicotine, 4-(Methylnitrosamino)-1-(3-pyridyl)-1-butanol, and 4-(methylnitrosamino)-1-(3-pyridyl)-1-butanone, have been identified in food products. Nitrosamines that alkylate and methylate are of particular concern due to their capacity to cause DNA damage in normal cells. Research has shown that rats exposed to nitrosamines from tobacco developed tumors in various organs, including the colon, nose, lung, mouth, liver, esophagus, pancreas, and breast (Moazeni *et al*., 2020).

DEN, a carcinogenic compound, is frequently used to induce tumor models in the respiratory system, skin, gastrointestinal tract, and liver. Administration via intraperitoneal injection or gavage at doses of 10 mg/kg of body weight leads to initial signs of liver toxicity, such as chronic inflammation and fibrosis. Higher doses exceeding 30 mg/kg of body weight initiate the induction, promotion, and progression of liver tumors (Tang *et al*., 2020). The tumor-inducing effects of DEN are linked to increased expression levels of G1/S-phase regulatory proteins, such as cyclin-dependent kinases, in hepatocytes. Additionally, DEN undergoes biotransformation, producing alkylating metabolites that cause DNA damage in hepatocytes. Reactive oxygen species (ROS) and reactive nitrogen species (RNS) generated during DEN metabolism disrupt the balance between free radical scavenging and production, inhibiting endogenous antioxidant enzymes and causing damage to cellular macromolecules, including proteins and polyunsaturated fatty acids (Memon *et al*., 2020).

HOTAIR, a long non-coding RNA associated with various cancers, including liver cancer, regulates gene expression by interacting with chromatin-modifying complexes, thus influencing cellular epigenetics (Price *et al*., 2021). Within the context of liver cancer, miR-124, a microRNA, controls cellular processes such as proliferation, invasion, and metastasis, and its dysregulation is associated with disease progression. The transmembrane receptor Notch1, which plays a crucial role in cell signaling for proliferation, differentiation, and apoptosis, has been implicated in the development of liver cancer due to abnormal activation of its pathway. Similarly, Jagged1, a Notch receptor ligand, contributes to liver cancer by activating the Notch pathway and promoting tumor growth, metastasis, and unfavorable patient prognosis. Ongoing research into the interactions and functions of these molecules in liver cancer reveals intricate molecular mechanisms that may present new targets for therapeutic interventions (Chen & Kong, 2022).

The leaf extract of *Nasturtium officinale* L. (NOLE) originates from the Brassicaceae family and is distributed worldwide, particularly in Eastern Europe, Northern Africa, and Asia. Thriving in humid to semi-humid climates, this plant blooms with pinkish-white flowers from July to September. NOLE consists of approximately 25-35% starch, 5% mucilage, 10% saccharose, 11% pectins, and various polyphenols such as catechin, daidzein, caffeic acid, pcoumaric acid, kaempferol, genistein, and isoquercitrin, alongside phytosterols, coumarins, asparagine, tannins, and scopoletin (Khudier *et al*., 2023). Traditionally, NOLE has been used as a seasoning in soups, teas, and vegetables, as well as a food additive, to alleviate conditions like dry coughs, flatulence, diabetes, hyperlipidemia, diarrhea, fever, and to enhance immunity against viruses and bacteria. In modern medicine, NOLE and its bioactive compounds are employed in treating cardiovascular diseases, exerting antimicrobial effects in respiratory tract infections, preventing urolithiasis, and modulating immunity and estrogenic effects (Saliani *et al*., 2023). Research indicates that NOLE acts as both an antioxidant and an inducer of apoptosis, enhancing the expression of the Glutathione-S-transferase (GST) gene by reducing DNA hyper-methylation, thus inhibiting proliferation in the prostate cancer cell line (PC-3) (Gorbanzadeh & Zaefizadeh, 2017). Additionally, NOLE enhances the expressions of TIMP-1 and TIMP-2, inhibiting MMP-2 and MMP-9, thereby restraining survival and metastasis in gastric cancer cell lines (AGS and MKN-45) (Matsushima *et al*., 2013). In our current investigation, we aim to evaluate the anti-tumor effects of NOLE against DEN-induced HCC in Wistar rats, focusing on anti-oxidative, anti-inflammatory, mitochondrial apoptosis, and HOTAIR/miR-124/Notch1 signaling pathways.

MATERIAL AND METHOD

Preparation of NOLE. The freshly harvested leaves of *Nasturtium officinale* L. weighing 4000 g were subjected to drying at 35 °C in a dark environment, following confirmation by a botanist. Subsequently, the dried leaves were ground into a powder using a soil grinder. The powdered leaves were then mixed with 70 % ethanol (30:70 distilled water (DW) / ethanol). After 72 h of incubation at 35 °C, the mixture underwent filtration through a paper filter, followed by compression using a rotary evaporator. The resulting extract, weighing 350 g, was stored at 4 °C (Kianbakht & Hashem-Dabaghian, 2019).

Experimental design. Fifty male Wistar rats, with an average weight of 180±30 g, were randomly divided into 5 groups (n=10/group). Before the study began, a 72-hour adaptation period was provided for the rats to adjust to the study conditions, including temperature, food, and water. Throughout the study, all rats were housed in propylene cages maintained at a temperature of 24±2 °C, with a relative humidity of 45±5 %, and subjected to a 12/12 dark/light cycle. Standard rat pellets and tap water were available ad libitum to all groups. The research protocol with animal experimentation was approved by the Scientific Ethics Committee of the First Affiliated Hospital of Zhejiang Chinese Medical University.

The normal group received an intraperitoneal injection of 500 µl PBS, while the HCC group received an intraperitoneal injection of 100 mg/kg DEN dissolved in 500 µl PBS. The co-treatment groups (DEN+100 and 200 NOLE) were orally administered DEN along with 100 and 200 mg/kg of NOLE, respectively. Additionally, the normal+200 NOLE group received 200 mg/kg of NOLE orally. The LD50 technique, along with preliminary studies and existing research on DEN and NOLE, was utilized to determine the effective dose of the non-toxic treatment. Administration of DEN and NOLE took place daily at fixed times, 9 am and 3 pm, respectively (Bazm *et al*., 2018).

LD_{50} for VAFE. The determination of the LD50 of NOLE was conducted using Lork's two-step method. Initially, nine rats were divided into three groups and administered doses of 5, 50, and 500 mg/kg of NOLE, respectively. These rats were then closely monitored for any signs of mortality or toxicity over a 24-hour period. Subsequently, another set of three rats per group received doses of 10, 100, and 1000 mg/kg of NOLE, respectively, and were similarly observed within the same timeframe. The LD50 was calculated using Lork's formula, which incorporates the highest safe dose (DS) and the lowest dose resulting in mortality (toxic dose, DT) observed during the monitoring period.

$$LD_{50} = (D_T \times D_S)^{1/2}$$ (Wang *et al*., 2023).

Serum levels of alkaline phosphatase (ALP), albumin (ALB), alanine aminotransferase (ALT), C-reactive protein (CRP), total protein (TP), aspartate aminotransferase (AST), and bilirubin (BIL). After the study was finished, rats were put to sleep using a combination of pre-anesthesia and anesthesia. This process involved the injection of 50 mg/kg of 2 % xylazine and 30 mg/kg of 10 % ketamine into the intraperitoneal area. Following this, blood samples were taken from the heart, and serum was separated through centrifugation. Next, the levels of AST, BIL, CRP, ALT, ALP, TP, and ALB in the serum were measured using ELISA kits from a commercial source, according to the guidelines provided by the manufacturer (Wang *et al*., 2023).

Serum glutathione peroxidase (GPx), catalase (CAT), and superoxide dismutase (SOD) activity. We employed a sandwich-based ELISA kit tailored for rodents, obtained from the Cusabio company in China, to measure the serum levels of glutathione peroxidase (GPx; Cat. No.: CSB-E12146r), catalase (CAT; Cat. No.: CSB-E13439r), and superoxide dismutase (SOD; Cat. No.: CSB-EL022397RA), adhering to the guidelines provided by the manufacturer (Wang *et al*., 2023).

Serum levels of nitric oxide (NO). The Griess colorimetric method was employed to evaluate serum nitric oxide (NO) levels, which serve as a vital indicator of lipid peroxidation and oxidative stress. In summary, 500 ml of serum samples were mixed with 6 mg of zinc oxide, thoroughly blended, and then centrifuged at 10,000 g for 15 min. The resulting supernatant was transferred to 500 ml of Griess solution. After an incubation period of 60 min at 37°C, the absorbance of the resulting mixture was measured using an ELISA reader (Stat Fax ELISA reader, model number: 303 microwell readers, from Awareness Technology company, United States) at wavelengths of 540 nm and 630 nm (Vargas-Maya *et al*., 2021).

Liver tissue thiol levels, total antioxidant capacity (FRAP levels), and lipid peroxidation levels (TBARS levels). One technique utilized to evaluate the total antioxidant capacity involves FRAP assessment. To summarize, 100 mg of liver tissue was homogenized at 4 °C, then combined with 200 µl of cold PBS. From this mixture, 100 µl was transferred to 10 µl of FRAP solution. After incubating the extract at 25 °C for 15 min and subsequent centrifugation at 12,000 g for 10 min, the absorbance of the resulting supernatant was measured at 593 nm using an ELISA reader (Stat Fax ELISA reader, model number: 303 microwell readers, from Awareness Technology company, United States).

Another method to quantify levels of lipid peroxidation involves assessing liver tissue TBARS. Initially, 100 µl of homogenized liver tissue mixture was combined with 100 µl of TBARS solution, followed by incubation at 37 °C for 30 min and centrifugation at 12,000 g for 5 min. The wavelength of the resulting supernatant was then measured at 593 nm using an ELISA reader.

For determining liver tissue thiol levels, which serve as a crucial tissue antioxidant index, 100 µl of homogenized liver tissue mixture was mixed with 20 µl of 5,5-dithio-bis-(2-nitrobenzoic acid) (DTNB), followed by incubation at 37 °C for 15 min and subsequent centrifugation at 12,000 g for 5 min. The wavelength of the supernatant was measured at 412 nm using an ELISA reader (Alam *et al*., 2023).

IL-10, IL-1β, TNF-α, and IL-6 serum levels. In order to evaluate the anti-inflammatory properties of VAFE extract, the concentrations of pro-inflammatory cytokines [TNF-α (Cat. No.: NBP2-DY410), IL-6 (Cat. No.: M6000B), and IL-1β (Cat. No.: RLB00)], along with the anti-inflammatory cytokine IL-10 (Cat. No.: R1000), were measured using sandwich-style ELISA kits designed for rodents, sourced from Novus Biologicals (United States). These assessments were conducted in accordance with the manufacturer's instructions (Alam *et al*., 2023).

Jagged1, miR-124, HOTAIR, and Notch1 genes expression. Liver tissue total RNA extraction was performed using EX6101-RNX Plus Solution (Cat. No.: EX6101-RNX; SinaClon BioScience, China). Initially, cell lysis was initiated by adding RNX Plus buffer, followed by the addition of 200 µl of chloroform. Subsequent centrifugation at 13,000 g for 15 min at 4 °C facilitated phase separation, resulting in a supernatant. This supernatant was then mixed with cold isopropanol (200 µl) and incubated on ice for 15 min before undergoing another round of centrifugation at 13,000 g for 15 min. Following this, 1 ml of 50 % ethanol was added to the samples, which were then centrifuged for 15 min at 13,000 g at 4 °C. The resulting pellet was finally re-suspended in 50 ml of distilled water and stored at -80 °C.

For cDNA synthesis, the Revert AidTM First Strand cDNA Synthesis Kit (Cat. No.: K1621; Fermentas, USA) was utilized, following the manufacturer's instructions. The sequences of HOTAIR, miR-124, Notch1, and Jagged1 genes were designed using gene runner software (Hastings Software, Hudson, United States). After the design phase, the genes underwent a blast search in the NCBI database (*https://www.ncbi.nlm.nih.gov/tools/primer-blast/*) for validation. The GAPDH gene was selected as the internal reference, and the primer sequences were as follows: GAPDH (forward: TGAAGGTCGGAGTCAACGG, reverse: AGAGTTAAAAGCAGCCCTGGTG), HOTAIR (forward: GGTAGAAAAAGCAACCACGAAGC, reverse: ACATAAACCTCTGTCTGTGAGTGCC), Jagged1 (forward: CGCCCTCTGAAAAACAGAAC, reverse: ACCCAAGCCACTGTTAAGACA), Notch1 (forward: CTGGACCCCATGGACATC, reverse: ACTGTACACAC TGCCGGTTG), and miR-124 (forward: GGAACCTTCT GAGTGCCTTAC, reverse: CCGTAAGTGGCGCACGG AAT). Gene amplification was performed using forward and reverse primers under 42 temperature cycles on a Corbett Rotor thermocycler, with each cycle encompassing 5 min at 70 °C as the annealing temperature. Relative expression levels of the genes were determined using the threshold cycle (Ct) of each gene, ΔΔCt, and the fold change formula: ΔΔCt = [(Ct sample - Ct GAPDH gene) - (Ct sample – Ct control)].

The fold formula change = $2^{-\Delta\Delta CT}$ (Chen *et al*., 2021).

Expression Jagged1, miR-124, HOTAIR, and Notch1 proteins in liver with western blotting. To assess the protein expression levels of HOTAIR, miR-124, Notch1, and Jagged1, Western blot analysis was performed. Initially, a homogenized liver tissue sample was prepared, with 100 mg of the sample combined with 50 µl of PBS and 100 µl of radio-immunoprecipitation assay buffer. Following centrifugation, 20 µl of loading buffer was added to a polyvinylidene fluoride (PVDF) membrane containing primary antibodies sourced from Abcam, UK, targeting HOTAIR (Cat. No. ab062614; 1:400), Notch1 (Cat. No. ab114178; 1:500), Jagged1 (Cat. No. ab152171; 1:500), and miR-124 (Cat. No. ab0616241; 1:500). Subsequently, the mixture was subjected to separation on an SDS polyacrylamide gel (10 %) using appropriate techniques. Following a 12-hour incubation at 4 °C, the membrane underwent additional incubation with an HRP-conjugated secondary antibody for 40 min at 37 °C. Finally, the protein bands' signals were captured and analyzed using Bio-Rad software, employing an enhanced chemiluminescence reagent from e-BLOT company, China. Further analysis was conducted using Image J software (Wang *et al*., 2020).

Immunohistochemistry (IHC) assay. Detection of p53-positive cells in liver tissues served as an indicator of apoptotic differentiation within tumor cells. Liver tissues underwent PBS washing and standard tissue processing, resulting in the creation of paraffin blocks. Sections measuring 5 µm were mounted on slides and subjected to overnight incubation at 95 °C with primary p53 antibodies (dilution 1:500; Cat. No.: GAF1355, R&D Systems, Inc., US). Subsequently, the slides were incubated for 1 h at 25 °C. Tween-20 was used as the washing buffer, and any residual antibodies were blocked with 5 % bovine serum albumin. The slides were then treated with 3 % hydrogen peroxide

(H_2O_2) for 20 min at 25 °C, followed by staining with 3,3'-diaminobenzidine (DAB). Hematoxylin was employed for counterstaining on all slides. An optical microscope (Model No. BX61TRF; Olympus, Japan), connected to Image J software, enabled examination of the slides at a magnification of 400X in ten randomly selected fields (Dhar *et al*., 2018).

Liver histopathology. Liver tissues underwent fixation in 10 % formalin for 72 h, followed by a gentle rinse with phosphate-buffered saline (PBS). After fixation, the samples were dehydrated in gradually increasing concentrations of ethanol, clarified in xylene, and embedded in paraffin wax. Sections measuring 5 µm were obtained from the paraffin blocks using a microtome (Model No. SM2010RV1.2 microtomes, LEICA, Germany) and then dried in an incubator at 37 ˚C. Slides were prepared for hematoxylin and eosin (H&E) staining. Histological examination of the slides was conducted using a light microscope at ×400 magnification. Images were captured using a calibrated light microscopic system (Model No. BX61TRF; Olympus, Japan) and processed using ImageJ software (Chen *et al*., 2020).

Statistical analysis approach. To compare the quantitative findings among the studied groups, statistical analysis was carried out using the one-way analysis of variance (ANOVA) followed by the Newman-Keuls *post hoc* test. A significance threshold of $p < 0.05$ indicated statistical significance. The normality and homogeneity of the data were assessed using the Kolmogorov-Smirnov test, with a p-value exceeding 0.05 indicating normal distribution and homogeneity. All results are presented as means ± standard deviation (SD). Data analysis was conducted using SPSS software (Ver. 16; IBM Inc, US), while GraphPad Prism software (Ver. 9; GraphPad Inc, US) was utilized for the graphical representation of the findings.

RESULTS

LD50 of NOLE. After a 24-hour monitoring period of the groups treated with NOLE, the results revealed a safe dose (Ds) at 500 mg/kg, while the toxic dose (D_T) was identified as 1000 mg/kg of NOLE. By applying Lork's formula, the calculated LD_{50} for NOLE was determined to be 707.2 mg/kg. This suggests that in animal studies, doses lower than the LD_{50} of NOLE can be used.

Body (BW) and liver (LW) weight. After analyzing the results concerning BW and LW, it was noted that in the DEN group, DEN caused a significant reduction in BW ($p < 0.05$) and a noticeable increase in LW ($p < 0.05$) compared to the normal group. Conversely, the administration of NOLE displayed a dose-dependent effect at 100 and 200 mg/kg in the DEN+100 and 200 mg/kg NOLE groups. This led to a significant weight increase in the rats ($p < 0.05$) and a considerable decrease in liver weight compared to the DEN group (Fig. 1A).

Effects of NOLE and DEN on serum liver biochemical parameters. After evaluating serum liver enzyme activities (ALT, AST, and ALP), it was observed that DEN significantly ($p < 0.05$) increased the activity levels of all three liver enzymes compared to the normal group. In the treatment groups (DEN+100 and 200 mg/kg NOLE), both demonstrated a significant reduction ($p < 0.05$) in the activity levels of all three enzymes compared to the DEN group (Fig. 1B).

Analysis of serum BIL and CRP data revealed a significant increase ($p < 0.05$) in both indicators within the DEN group compared to the control group. Notably, NOLE exhibited a dose-dependent effect in decreasing ($p < 0.05$) the levels of these serum indicators compared to the DEN group. Assessment of serum ALB and TP levels across the groups also showed that DEN significantly ($p < 0.05$) decreased the levels of both markers compared to the control group. Conversely, in the DEN+200 NOLE treatment group, there was a significant increase ($p < 0.05$) in the levels of both markers compared to the DEN group (Fig. 1C).

Thiol, FRAP, and TBARS levels in liver. Thiol, FRAP, and TBARS levels were essential indicators of overall antioxidant capacity and lipid peroxidation. The results showed that DEN significantly ($p < 0.05$) reduced the levels of all three factors in the tissues compared to the normal group. Conversely, NOLE, known for its potent antioxidant properties, exhibited a dose-dependent increase in the levels of these factors compared to the DEN group. This increase was statistically significant ($p < 0.05$) at the dosage of 200 mg/kg (within the DEN+200 NOLE group) compared to the DEN group (Fig. 2A).

Serum GPx, CAT, and SOD activity alongside serum NO levels. DEN, through the induction of free radical production, resulted in a notable increase in serum NO levels compared to the normal group. Conversely, NOLE demonstrated a dose-dependent decrease in NO levels compared to the DEN group. This reduction was statistically significant ($p < 0.05$) at the dosage of 200 mg/kg (within the DEN+200 NOLE group). Additionally, DEN substantially reduced the serum activity of all three antioxidant enzymes compared to the control group. In contrast, NOLE elevated the serum levels of all three enzymes in a dose-dependent manner compared to the control group, with a statistically significant increase ($p < 0.05$) observed at the dosage of 200 mg/kg (within the DEN+200 NOLE group) compared to the DEN group (Fig. 2B).

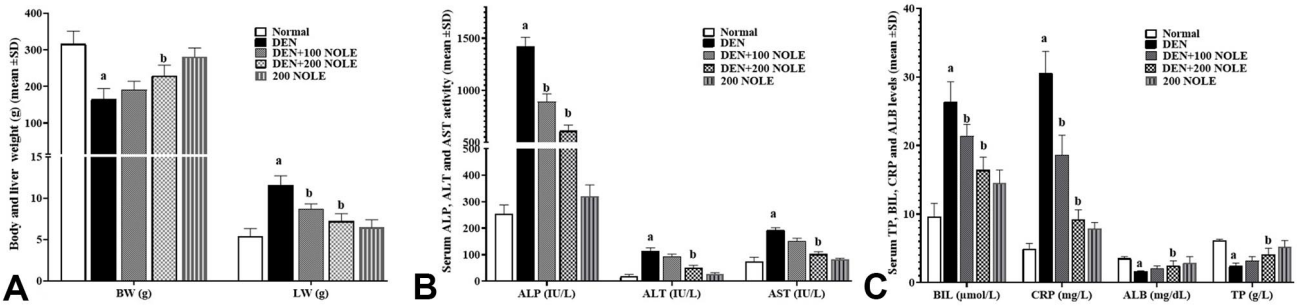

Fig. 1. (A) Rats body (BW) and liver (LW) (g) weight, (B) Serum activity of alanine aminotransferase (ALT), aspartate aminotransferase (AST), and alkaline phosphatase (ALP) enzymes (IU/L), and (C) serum levels of albumin (ALB) (mg/dL), total protein (TP) (g/L), and bilirubin (BIL) (μmol/L), C reactive protein (CRP) (mg/L) in experimental groups (means ± SD; n=10/group). [a]($p<0.05$) DEN *vs.* normal groups; [b]($p<0.05$) DEN+100 and 200 NOLE treated *vs*. DEN groups.

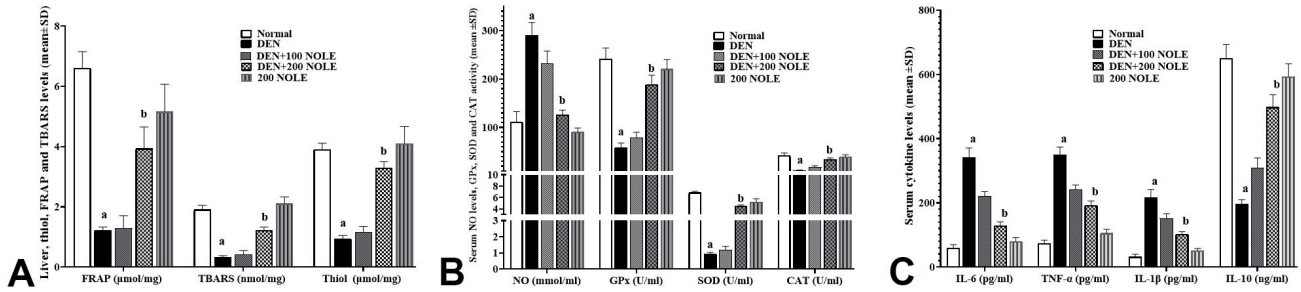

Fig. 2. (A) liver tissue levels of TBARS (nmol/mg) and FRAP (μmol/mg), (B) Serum levels of NO (mmol/ml), alongside the mean serum activity of SOD, CAT, and GPx (U/ml), and (C) Serum levels of IL-1β, TNF-α, IL-6 (pg/ml), and IL-10 (ng/ml) (means ± SD; n=10/group) in experimental groups. [a]($p<0.05$) DEN *vs.* normal groups; [b]($p<0.05$) DEN+100 and 200 NOLE treated *vs*. DEN groups.

Serum levels of TNF-α, IL-10, IL-6, and IL-1β. By instigating inflammatory responses, DEN increased the concentration of pro-inflammatory cytokines and impeded the activity of systemic anti-inflammatory cytokines. Consequently, there was a significant elevation ($p < 0.05$) in the serum levels of all three pro-inflammatory cytokines (TNFα, IL-1β, and IL-6) compared to the normal group, while the level of IL-10 notably decreased. However, the findings of the study revealed the potent anti-inflammatory properties of NOLE. It progressively raised the serum levels of IL-10 and decreased the levels of all three pro-inflammatory cytokines (TNF-α, IL-1β, and IL-6) compared to the DEN group. These changes were considered statistically significant ($p < 0.05$) at the dosage of 200 mg/kg (within the DEN+200 NOLE group) of this botanical agent compared to the control group (Fig. 2C).

Expression of liver HOTAIR, miR-124, Notch1, and Jagged1 genes. Analysis of gene expression associated with proliferation, differentiation, and apoptosis pathways indicated that DEN treatment significantly reduced the expression of HOTAIR, Notch1, and Jagged1 while increasing miR-124 expression in hepatocytes compared to the normal group ($p < 0.05$). In the DEN+100 NOLE group, there was an upregulation in HOTAIR, Notch1, and Jagged1 expression and a downregulation in miR-124 expression compared to the DEN group, although these changes were not statistically significant ($p > 0.05$). The most notable changes were observed in the DEN+200 NOLE group, where HOTAIR, Notch1, and Jagged1 expression significantly increased while miR-124 expression significantly decreased compared to the DEN group ($p < 0.05$) (Fig. 3A).

Expression of liver HOTAIR, miR-124, Notch1, and Jagged1 proteins. To comprehensively evaluate the impact of DEN on liver pathways associated with proliferation, differentiation, and apoptosis, we investigated the protein expression levels of HOTAIR, miR-124, Notch1, and Jagged1. The results of this analysis revealed a significant decrease ($p < 0.05$) in the protein expression of HOTAIR, Notch1, and Jagged1, accompanied by a significant increase ($p < 0.05$) in the protein expression of miR-124 compared to the healthy group. Conversely, in the DEN+100 NOLE group, there was an increase in the protein expression of HOTAIR, Notch1, and Jagged1, along with a decrease in the protein expression of miR-124 compared to the DEN group. However, these changes did not reach statistical significance ($p > 0.05$). The most noteworthy alterations were observed in the DEN+200 NOLE group, where there was a significant increase ($p < 0.05$) in the protein expression of HOTAIR, Notch1, and Jagged1, while a significant decrease ($p < 0.05$) was observed in the protein expression of miR-124 compared to the DEN group (Fig. 3B,C).

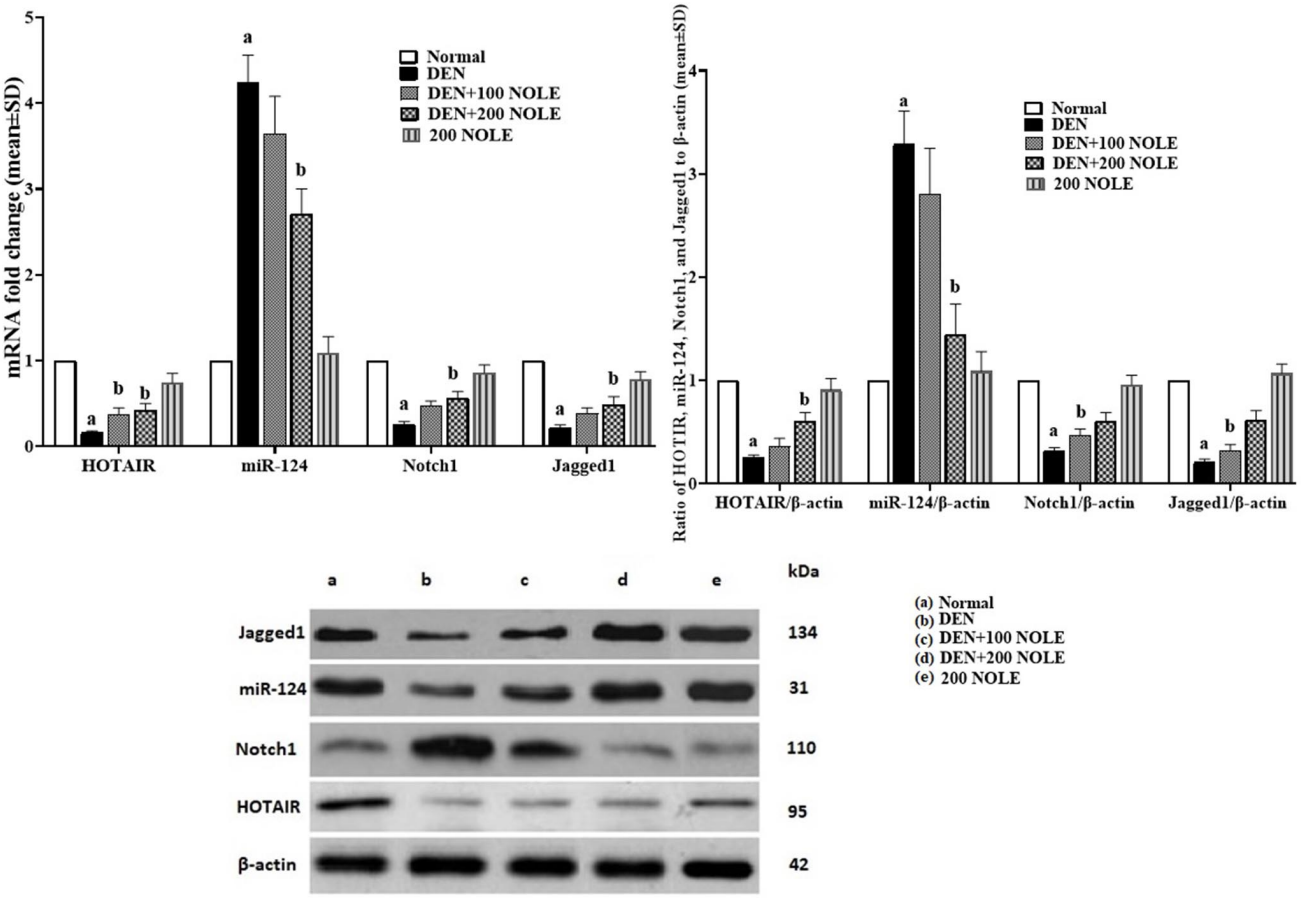

Fig. 3. (A) HOTAIR, miR-124, Notch1, and Jagged1 genes expression and (B, C) HOTAIR, miR-124, Notch1, and Jagged1 proteins expression in liver (means ± SD; n=10/group) in experimental groups. [a](p<0.05) DEN *vs.* normal groups; [b](p<0.05) DEN+100 and 200 NOLE treated *vs*. DEN groups.

Liver p53 positive hepatocytes. An examination of the results regarding the percentage of p53-positive cells revealed that DEN caused a significant increase ($p < 0.05$) in the proportion of these cells compared to the normal group. Additionally, the groups treated with only 100 and 200 mg/kg of NOLE extract showed improvements in apoptotic indices (reduction in p53-positive cells) compared to the DEN group. Specifically, the decrease in the percentage of p53-positive cells in the DEN+200 NOLE group was statistically significant compared to the DEN group (Fig. 4).

Liver histopathological evaluations. In the histopathological analysis of liver tissue in the studied groups, it was observed that DEN induced the formation of hepatic nodules (HN) characterized by lymphocytic infiltration (LI) and degenerated hepatocytes (D) neighboring the necrotic tissue. In this specific group, the typical hepatic triad (HT) and hepatic lobule (HL) were absent, while congestion (CO) and dilation of the central venule (CV) were evident. In the DEN+100 and 200 NOLE groups, the restoration of hepatic lobules to a normal state was observed, accompanied by a significant reduction in lymphocytic infiltration. Furthermore, the presence of hepatic nodules was no longer detectable in the liver, and the alignment of hepatocytes (H) adjacent to the liver sinusoids (S) was clearly visible. These changes appeared to be dose-dependent, with the most notable improvement in tissue structure observed in the DEN+200 NOLE group (Fig. 5).

DISCUSSION

The results of this study underscore the effectiveness of NOLE in maintaining the proper functioning of hepatocytes through antioxidant, anti-inflammatory, and anti-apoptotic mechanisms. Additionally, NOLE shows promise in regulating the HOTAIR/miR-124/Notch1 axis associated with DEN-induced HCC, thereby protecting against tumorigenic pathways in hepatocytes.

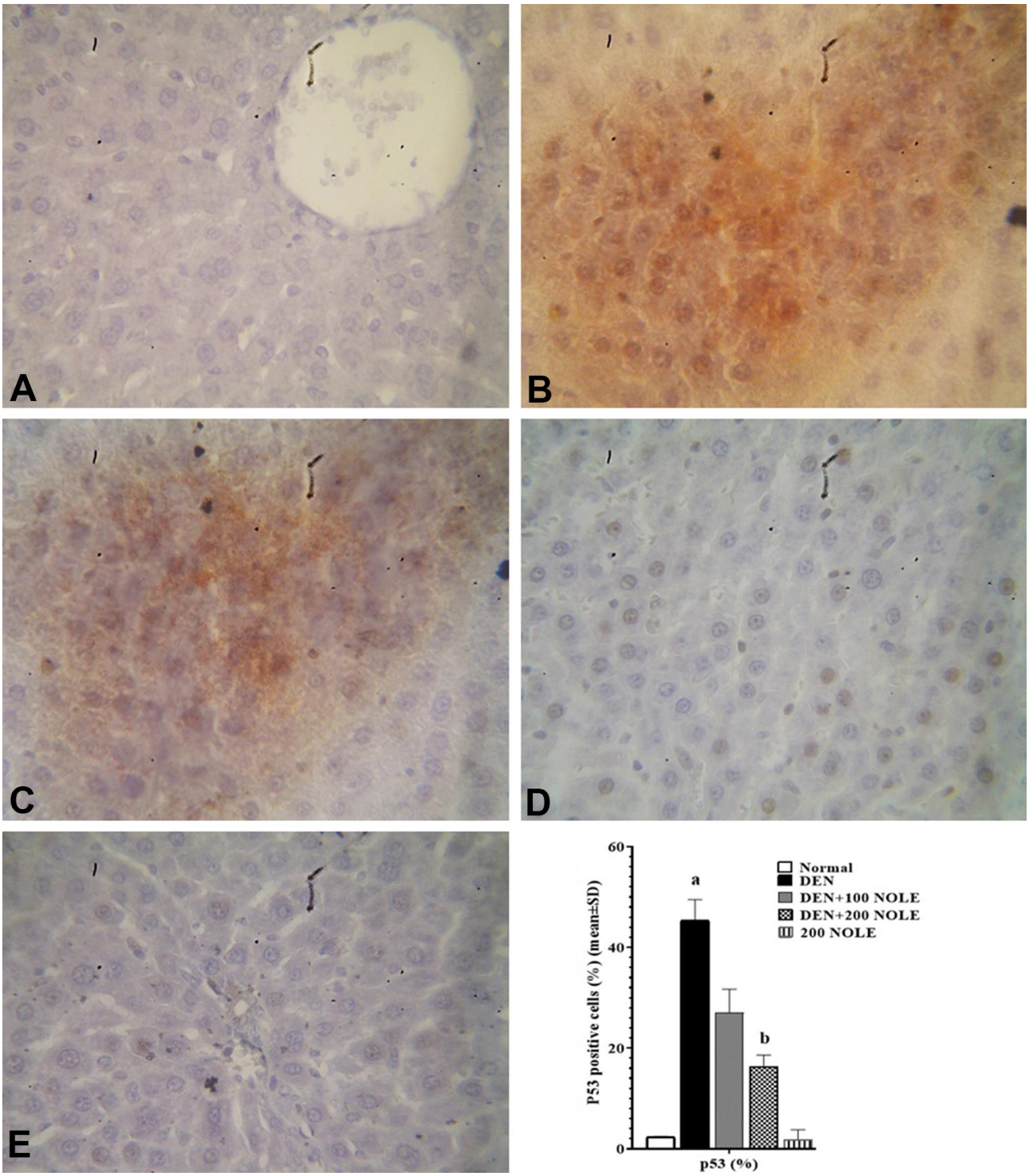

Fig. 4. p53 positive cells (%) in liver tissue by immunohistochemistry (n=10 rat/group, data are "means ± SD) (means ± SD; n=10/group) in normal (a), DEN (b), DEN+100 NOLE (c), DEN+200 NOLE (d), and 200 NOLE (× 100 with Scale bar = 200 μm). [a](p<0.05) DEN vs. normal groups; [b](p<0.05) DEN+100 and 200 NOLE treated *vs.* DEN groups.

DEN induced HCC. DEN affects various pathways involved in apoptosis, autophagy, proliferation, and differentiation of liver parenchymal cells. Among these pathways, Arboatti *et al*. (2019), indicate that DEN

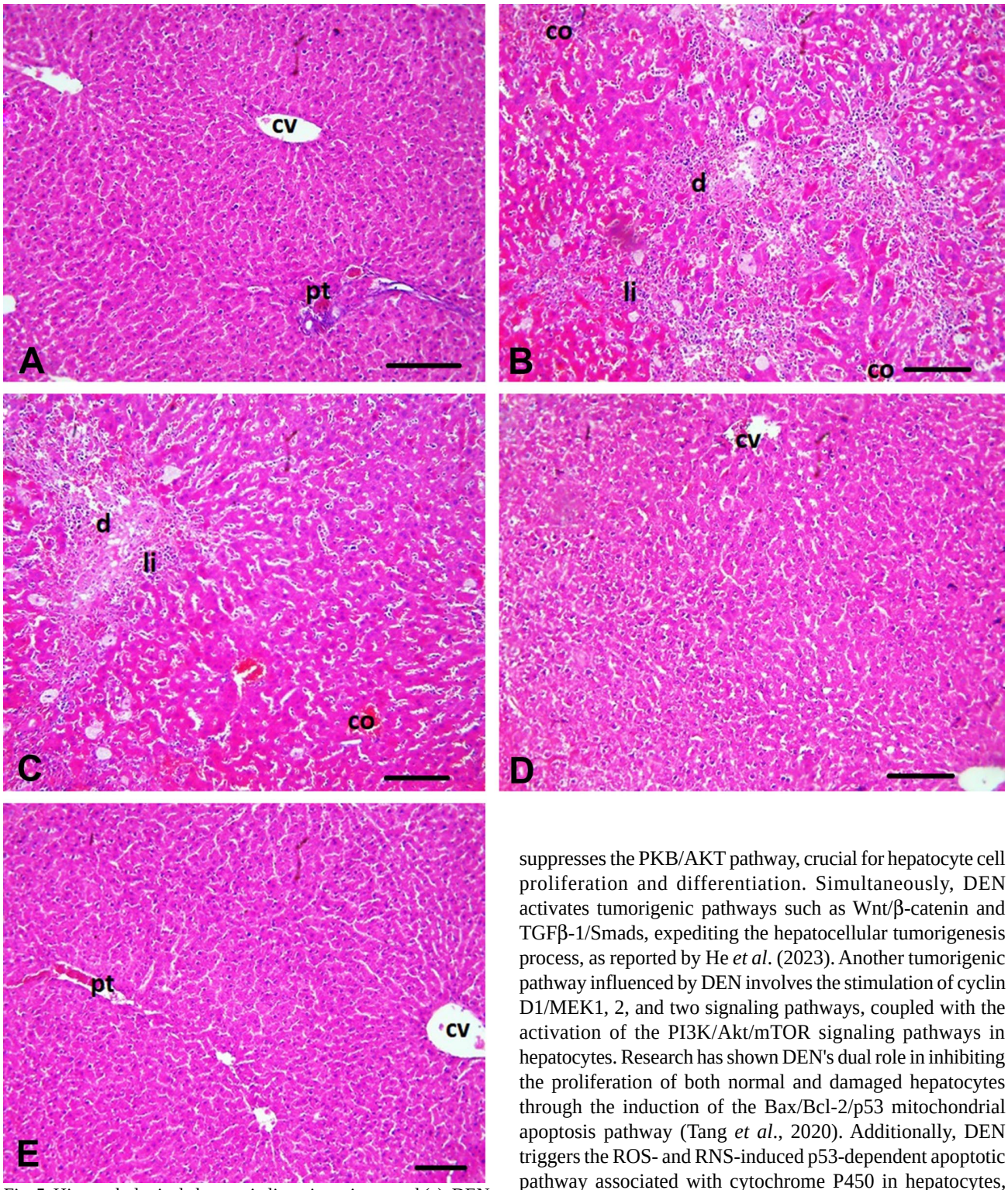

Fig. 5. Histopathological changes in liver tissue in normal (a), DEN (b), DEN+100 NOLE (c), HCC+200 NOLE (d), and 200 NOLE (H & E, × 100 with Scale bar = 200 μm). Congestion (CO), hepatic nodules (HN), lymphatic infiltration (LI), central venule (CV), hepatic degeneration (D), hepatic sinusoid's (S), normal hepatic lobule (HL) and hepatic triad (HT), and normal hepatocytes (H).

suppresses the PKB/AKT pathway, crucial for hepatocyte cell proliferation and differentiation. Simultaneously, DEN activates tumorigenic pathways such as Wnt/β-catenin and TGFβ-1/Smads, expediting the hepatocellular tumorigenesis process, as reported by He *et al*. (2023). Another tumorigenic pathway influenced by DEN involves the stimulation of cyclin D1/MEK1, 2, and two signaling pathways, coupled with the activation of the PI3K/Akt/mTOR signaling pathways in hepatocytes. Research has shown DEN's dual role in inhibiting the proliferation of both normal and damaged hepatocytes through the induction of the Bax/Bcl-2/p53 mitochondrial apoptosis pathway (Tang *et al*., 2020). Additionally, DEN triggers the ROS- and RNS-induced p53-dependent apoptotic pathway associated with cytochrome P450 in hepatocytes, initiating the apoptotic cascade. This cascade involves the activation of initiator caspases, such as caspases 8 and 9, followed by the activation of effector caspases, including caspases 3 and 6, prompted by the release of cytochrome c from mitochondria (Kamel & Lamsabhi, 2021).

Studies reveal that DEN, via STAT3, P38, JNK, and JAK signaling pathways, along with cyclooxygenase-2 (COX-2), IGF-2, cyclin D1, and mutation, induces hepatocyte necrosis and apoptosis, triggering the secretion of growth factors such as EGF and TGF-β, and subsequent tissue fibrosis and neoangiogenesis (Shang *et al*., 2018). The study results also indicate that DEN reduces antioxidant capacity (FRAP) and increases lipid peroxidation and liver proteins (TBARS and thiol) by inhibiting antioxidant enzymes (GPx, SOD, and CAT). Elevated ROS and RNS levels correlate with changes in liver functional indices (ALT, ALB, TP, CRP, AST, BIL, and ALP). In a separate study, Pradeep *et al*. (2010), demonstrated DEN's inhibition of GPx, SOD, LPO, CAT, and enzyme activities, resulting in elevated serum NO and hepatic MDA levels, indicating the development of oxidative stress (Shahin *et al*., 2018). Additionally, DEN increased serum liver enzyme levels (ALT, AST, and ALP), as well as BIL and CRP levels, disrupting the physiological function of hepatocytes. C-reactive protein (CRP), a significant inflammatory marker, rises in response to liver parenchymal damage, serving as a crucial indicator in animal studies. CRP in animal/human models can induce proinflammatory and inflammatory cytokines, particularly TNF-a and IL-6, through the p38 MAPK pathway, emphasizing the inflammatory phase (Zaahkouk *et al*., 2019).

DEN induces the release of proinflammatory cytokines (such as TNF-α, IL-22, and IL-6) while inhibiting anti-inflammatory cytokines (IL-4 and IL-10), thereby reinforcing various inflammatory pathways involving Kupffer cells, liver lymphocytes, and damaged cells (Lyngdoh *et al*., 2023). These cytokines contribute to necrotic and apoptotic cascades in various tissues, including the liver. The HOTAIR/miR-124/Notch1 axis, a crucial intracellular pathway, is influenced by DEN, regulating the growth, metabolism, motility, and proliferation of tumor cells. DEN reinforces the NF-κB/COX-2 pathway through the HOTAIR/miR-124/Notch1 axis and the Nrf-2/HO-1 axis, impacting hepatocyte function and liver indices following tumorigenesis and nodule formation (Sahin *et al*., 2014). The study also highlights DEN's involvement in inflammatory pathways (elevation of IL-6, IL-1β, and TNF-a) and the stimulation of the HOTAIR/miR-124/Notch1 axis.

NOLE ameliorates DEN-induced HCC. The results of this study indicate that NOLE exhibited dose-dependent improvements in hepatocyte function while maintaining their normal structure through antitumor, anti-inflammatory, and antioxidant pathways. NOLE effectively reduced levels of liver enzymes (ALT, AST, and ALP), BIL, and CRP, while increasing ALB and TP levels in a dose-dependent manner, with notable effects observed in the DEN + 200 NOLE group. Moreover, NOLE extract, particularly at 200 mg/kg (in the DEN+200 NOLE treatment group), suppressed inflammatory pathways (characterized by decreased levels of IL-6, IL-1b, and TNF-a, along with an increase in IL-10) and mitigated oxidative stress (evidenced by increased activity of GPx, SOD, and CAT, and decreased nitric oxide levels) induced by DEN.

Studies indicate that NOLE, functioning as an antioxidant and apoptotic inducer, increases Glutathione-S-transferase (GST) gene expression by alleviating DNA hyper-methylation, thus inhibiting proliferation of the prostate cancer cell line (PC-3) (Gorbanzadeh & Zaefizadeh, 2017). Matrix metalloproteinases (MMPs) play a crucial role in tumor cell invasion and metastasis by breaking down extracellular matrix (ECM) proteins like collagen, laminin, proteoglycan, fibronectin, and elastin. The endogenous tissue inhibitor of metalloproteinase (TIMP) counteracts MMP activity, hindering metastasis and invasion (Holmberg *et al*., 2013). Notably, NOLE extract enhances the expressions of TIMP-1 and 2, leading to inhibition of MMP-2 and 9, thereby restraining survival and metastasis of gastric cancer cell lines (AGS and MKN-45) (Matsushima *et al*., 2013).

Multidrug resistance (MDR) remains a significant challenge in chemotherapy, attributed to various mechanisms including activation of detoxifying systems, reduced drug uptake, activation of DNA repair mechanisms, and increased drug efflux mediated by ATP-binding cassette (ABC) transporters, notably ABCCs or multidrug resistance proteins (MRPs) (Cole., 2014; Ruan *et al*., 2020). NOLE demonstrates potential in overcoming MDR by enhancing the efficacy of chemotherapy drugs on gastric cancer cell lines (AGS and MKN-45), suppressing their growth and viability through downregulation of MRP-1 expression (Esmaeili *et al*., 2021). Comparative analysis of NOLE on human HL60 and ???116 tumor cell lines reveals its antitumor effects, attributed to anthocyanin content, particularly delphinidin, which induces tumor cell suppression and apoptosis (Karcheva-Bahchevanska *et al*., 2017). In a study by Muceniece *et al*. (2019), on the protective effects of NOLE against diazinon-induced hepatotoxicity, the plant extract showed a reduction in hepatic enzyme levels (ALT, AST, and ALP) while protecting liver structure and function against oxidative damage through stimulation of endogenous antioxidant enzymes (GPx, SOD, and CAT) (Muceniece *et al*., 2019). Akbari Bazm *et al*. (2020) investigated the protective effects of NOLE against oxymetholone-induced testicular toxicity in rats, revealing

its ability to decrease tissue MDA, thiol, and NO levels while enhancing GPx and SOD activity.

The interconnected elements of hepatic physiology and pathology encompass the HOTAIR/miR-124/Notch1 axis in hepatocytes, the insulin pathway, and liver cancer. HOTAIR, a long non-coding RNA (lncRNA), miR-124, a microRNA, along with Notch1, a transmembrane receptor, intricately regulate cellular processes in hepatocytes such as proliferation and differentiation, with their dysregulation implicated in the progression of liver cancer (Price *et al.*, 2021). The complex interactions within this axis involve HOTAIR potentially acting as a sponge for miR-124, resulting in increased Notch1 expression, which contributes to suppressing HCC. The insulin pathway governs glucose and lipid metabolism, with insulin resistance and hyperinsulinemia associated with hepatocarcinogenesis by promoting cell proliferation and inhibiting apoptosis (Chen & Kong, 2022). NOLE effectively modulated miR-124 by enhancing the HOTAIR/Notch1/Jagged1 axis, thereby impeding tumor cell proliferation and differentiation. Moreover, by reinforcing the HOTAIR/Notch1/Jagged1 antitumor pathway, NOLE induced apoptosis in hepatocytes.

CONCLUSION

In summary, our study emphasizes the potential of NOLE as a protective agent against DEN-induced HCC. Through a thorough examination of biochemical, molecular, and antioxidant pathways, coupled with its influence on the HOTAIR/miR-124/Notch1 axis pathway, we have identified significant therapeutic effects of NOLE. Our results demonstrate that NOLE administration effectively regulated liver function indices, enhanced antioxidant status, and attenuated inflammatory cytokine levels in HCC rats. Additionally, NOLE exhibited the capacity to modulate gene and protein expressions associated with HCC progression, particularly by reducing HOTAIR and Notch1 while elevating miR-124. This modulation effectively countered the activation of the Notch1/Jagged1 signaling pathway induced by HOTAIR, highlighting the potential of NOLE as an anticancer agent in DEN-induced HCC. However, further *in vivo* and *in vitro* investigations are essential to fully elucidate the anticancer properties of NOLE.

Ethical Approval. The experimental protocols of this study were approved by The First Affiliated Hospital of Zhejiang Chinese Medical University ethics committee.

Contributions. Huichao Feng and Sheng Zheng are co-first authors, they contributed equally to this work.

FENG, H.; ZHENG, S.; YANG, J.; MAO, X.; LIU, T.; ZHANG, Q. & CHEN, Y. Exploración de las propiedades anticancerígenas de *Nasturtium officinale* L. a través de la vía HOTAIR/miR-124/Notch1 en el carcinoma hepatocelular de rata: Una investigación utilizando métodos bioquímicos, moleculares, inmuno-histoquímicos e histopatológicos. *Int. J. Morphol., 42(5)*:1361-1372, 2024.

RESUMEN: Este estudio tuvo como objetivo explorar el potencial del extracto de hojas de *Nasturtium officinale* L. (NOLE) para proteger los hepatocitos contra el carcinoma hepatocelular (HCC) inducido por N-dietilnitrosamina (DEN) mediante la investigación de sus efectos sobre las vías bioquímicas, moleculares y antioxidantes. El estudio también profundizó en el papel de NOLE en la modulación de la vía del eje HOTAIR/miR-124/Notch1. En este estudio, 50 ratas Wistar se dividieron en cinco grupos (n=10/grupo): ratas normales, inducidas por HCC (100 mg/kg de DEN), ratas con HCC tratadas con 100 y 200 mg/kg de DEN + NOLE y ratas normales tratadas con 200 mg/kg de NOLE. Al concluir el estudio, se midieron los niveles séricos de marcadores de función hepática (como albúmina, proteína total, bilirrubina, proteína C reactiva, ALT, AST y ALP), citoquinas inflamatorias (IL-6, IL-1β, IL-10 y TNF-α) y parámetros oxidativos [incluidos los niveles de glutatión peroxidasa (GPx), superóxido dismutasa (SOD), catalasa (CAT) y óxido nítrico (NO)]. Se midieron los niveles de los genes y proteínas HOTAIR, miR-124, Notch1 y Jagged1 en el tejido hepático. Se utilizó análisis inmunohistoquímico para evaluar las células P53 positivas en los hepatocitos del hígado. La administración de DEN provocó alteraciones significativas en el peso corporal y hepático, las enzimas hepáticas séricas, los niveles de antioxidantes, los marcadores inflamatorios y la expresión de genes/proteínas relacionadas con el eje HOTAIR/miR-124/Notch1 en las vías hepáticas. NOLE exhibió efectos dependientes de la dosis para mitigar estos cambios, en particular mejorando el peso, la salud del hígado, la capacidad antioxidante y las respuestas inflamatorias, especialmente en la dosis de 200 mg/kg. Las evaluaciones histopatológicas revelaron mejoras estructurales en el tejido hepático con el tratamiento NOLE. En conclusión, nuestro estudio destaca el potencial de NOLE para ejercer efectos anticancerígenos contra el CHC inducido por DEN.

PALABRAS CLAVE: *Nasturtium officinale* L.; N-dietilnitrosamina; AIRE CALIENTE; Hígado; Carcinoma hepatocelular.

REFERENCES

Akbari Bazm, M.; Goodarzi, N.; Shahrokhi, S. R. & Khazaei, M. The effects of hydroalcoholic extract of *Vaccinium arctostaphylos* L. on sperm parameters, oxidative injury and apoptotic changes in oxymetholone-induced testicular toxicity in mouse. *Andrologia, 52(3)*:e13522, 2020.

Alam, R.; Ahsan, H. & Khan, S. The role of malondialdehyde (MDA) and ferric reducing antioxidant power (FRAP) in patients with hypertension. *Mol. Cell. Biomed. Sci., 7(2)*:58-64, 2023.

Arboatti, A. S.; Lambertucci, F.; Sedlmeier, M. G.; Pisani, G.; Monti, J.; Álvarez, M. L. & Carnovale, C. E. Diethylnitrosamine enhances hepatic tumorigenic pathways in mice fed with high fat diet (Hfd). *Chem. Biol. Interact., 303*:70-8, 2019.

Bazm, M. A.; Khazaei, M.; Ghanbari, E. & Naseri, L. Protective effect of *Vaccinium arctostaphylos* L. fruit extract on gentamicin-induced nephrotoxicity in rats. *Comp. Clin. Pathol., 27*:1327-34, 2018.

Chen, L. & Kong, C. LINC00173 regulates polycystic ovarian syndrome progression by promoting apoptosis and repressing proliferation in ovarian granulosa cells via the microRNA-124-3p (miR-124-3p)/jagged canonical Notch ligand 1 (JAG1) pathway. *Bioengineered, 13(4)*:10373-85, 2022.

Chen, M.; Zhang, B.; Topatana, W.; Cao, J.; Zhu, H.; Juengpanich, S.; Mao, Q.; Yu, H. & Cai, X. Classification and mutation prediction based on histopathology H&E images in liver cancer using deep learning. *NPJ Precis. Oncol., 4*:14, 2020.

Chen, S.; Wang, J.; Fang, Q.; Dong, N.; Fang, Q.; Cui, S. W. & Nie, S. A polysaccharide from natural c regulates the intestinal immunity and gut microbiota in mice with cyclophosphamide-induced intestinal injury. *Food Funct., 12(14)*:6271-82, 2021.

Dhar, D.; Antonucci, L.; Nakagawa, H.; Kim, J. Y.; Glitzner, E.; Caruso, S.; Shalapour, S.; Yang, L.; Valasek, M. A.; Lee, S.; *et al*. Liver cancer initiation requires p53 inhibition by CD44-enhanced growth factor signaling. *Cancer Cell, 33(6)*:1061-1077.e6, 2018.

Garcia-Lezana, T.; Lopez-Canovas, J. L. & Villanueva, A. Signaling pathways in hepatocellular carcinoma. *Adv. Cancer Res., 149*:63-101, 2021.

Gorbanzadeh, E. & Zaefizadeh, M. Inhibitory effects of *Vaccinium arctostaphylos* extract on prostate cancer cells. *J. Ardabil Univ. Med. Sci., 17(4)*:487-96, 2017.

He, J., Han, J.; Lin, K.; Wang, J.; Li, G.; Li, X. & Gao, Y. PTEN/AKT and Wnt/b-catenin signaling pathways regulate the proliferation of Lgr5+ cells in liver cancer. *Biochem. Biophys. Res. Commun., 683*:149117, 2023.

Kamel, E. M. & Lamsabhi, A. M. Water biocatalytic effect attenuates cytochrome P450-mediated carcinogenicity of diethylnitrosamine: A computational insight. *Org. Biomol. Chem., 19(41)*:9031-2, 2021.

Karcheva-Bahchevanska, D.; Lukova, P.; Nikolova, M.; Mladenov, R. & Iliev, I. Therapeutic effects of anthocyannins from *Vaccinium genus* L. *Int. J. Med. Res. Pharm., 4*:4-19, 2017.

Khudier, M. A.; Hammadi, H. A.; Atyia, H. T.; Al-Karagoly, H.; Albukhaty, S.; Sulaiman, G. M. & Mahood, H. B. Antibacterial activity of green synthesized selenium nanoparticles using *Vaccinium arctostaphylos* (L.) fruit extract. *Cogent Food Agric., 9(1)*:2245612, 2023.

Lyngdoh, A.; Baruah, T. J.; Sharan, R. N. & Kma, L. Inhibitory potential of Apium graveolens L. extract on inflammation in diethylnitrosamine-induced hepatocellular carcinoma in mice. *Pharmacognosy Magazine, 19(3)*:736-50, 2023.

Matsushima, M.; Suzuki, T.; Masui, A.; Mine, T. & Takagi, A. Cranberry extract suppresses interleukin-8 secretion from stomach cells stimulated by *Helicobacter pylori* in every clinically separated strain but inhibits growth in part of the strains. *J. Funct. Foods, 5(2)*:729-35, 2013.

Memon, A.; Pyao, Y.; Jung, Y.; Lee, J. I. & Lee, W. K. A modified protocol of diethylnitrosamine administration in mice to model hepatocellular carcinoma. *Int. J. Mol. Sci., 21(15)*:5461, 2020.

Moazeni, M.; Heidari, Z.; Golipour, S.; Ghaisari, L.; Sillanpää, M., & Ebrahimi, A. Dietary intake and health risk assessment of nitrate, nitrite, and nitrosamines: a Bayesian analysis and Monte Carlo simulation. *Environ. Sci. Pollut. Res. Int., 27(36)*:45568-80, 2020.

Muceniece, R.; Klavins, L.; Kviesis, J.; Jekabsons, K.; Rembergs, R.; Saleniece, K. & Klavins, M. Antioxidative, hypoglycaemic and hepatoprotective properties of five *Vaccinium spp*. berry pomace extracts. *J. Berry Res., 9(2)*:267-82, 2019.

Price, R. L.; Bhan, A. & Mandal, S. S. HOTAIR beyond repression: In protein degradation, inflammation, DNA damage response, and cell signaling. *DNA Repair, 105*:103141, 2021.

Saliani, N.; Kouhsari, S. M. & Izad, M. The potential hepatoprotective effect of *Vaccinium arctostaphylos* L. fruit extract in diabetic rat. *Cell J., 25(10)*:717-26, 2023.

Shang, N.; Bank, T.; Ding, X.; Breslin, P.; Li, J.; Shi, B. & Qiu, W. Caspase-3 suppresses diethylnitrosamine-induced hepatocyte death, compensatory proliferation and hepatocarcinogenesis through inhibiting p38 activation. *Cell Death Dis., 9(5)*:558, 2018.

Singal, A. G.; Kanwal, F. & Llovet, J. M. Global trends in hepatocellular carcinoma epidemiology: implications for screening, prevention and therapy. *Nat. Rev. Clin. Oncol., 20(12)*:864-84, 2023.

Stanfill, S. B.; Hecht, S. S.; Joerger, A. C.; González, P. J.; Maia, L. B.; Rivas, M. G.; Moura, J. J. G.; Gupta, A. K.; Le Brun, N. E.; Crack, J. C.; *et al*. From cultivation to cancer: formation of N-nitrosamines and other carcinogens in smokeless tobacco and their mutagenic implications. *Crit. Rev. Toxicol., 53(10)*:658-701, 2023.

Tang, Y.; Cao, J.; Cai, Z.; An, H.; Li, Y.; Peng, Y.; Chen, N.; Luo, A.; Tao, H. & Li, K. Epigallocatechin gallate induces chemopreventive effects on rats with diethylnitrosamine-induced liver cancer via inhibition of cell division cycle 25A. *Mol. Med. Rep., 22(5)*:3873-85, 2020.

Thylur, R. P.; Roy, S. K.; Shrivastava, A.; LaVeist, T. A.; Shankar, S. & Srivastava, R. K. Assessment of risk factors, and racial and ethnic differences in hepatocellular carcinoma. *JGH Open, 4(3)*:351-9, 2020.

Vargas-Maya, N. I.; Padilla-Vaca, F.; Romero-González, O. E.; Rosales-Castillo, E. A. S.; Rangel-Serrano, Á.; Arias-Negrete, S. & Franco, B. Refinement of the Griess method for measuring nitrite in biological samples. *J. Microbiol. Methods, 187*:106260, 2021.

Wang, Q.; Li, X.; Ren, S.; Su, C.; Li, C.; Li, W.; Yu, J.; Cheng, N. & Zhou, C. HOTAIR induces EGFR-TKIs resistance in non-small cell lung cancer through epithelial-mesenchymal transition. *Lung Cancer, 147*:99-105, 2020.

Wang, Z.; Jiang, X.; Zhang, L. & Chen, H. Protective effects of Althaea officinalis L. extract against N-diethylnitrosamine-induced hepatocellular carcinoma in male Wistar rats through antioxidative, anti-inflammatory, mitochondrial apoptosis and PI3K/Akt/mTOR signaling pathways. *Food Sci. Nutr., 11(8)*:4756-72, 2023.

Zaahkouk, S. A.; Mehany, A.; El-Shamy, S. A. & EL-Sharkawy, S. M. Hematological and biochemical changes in rats induced with diethyl nitrosamine and the hepatoprotective role of some antioxidants. *Egypt. Acad. J. Biol. Sci. B. Zool., 11(2)*:51-64, 2019.

Corresponding author:
Yaqin Chen
Department of Pediatrics
The First Affiliated Hospital of Zhejiang Chinese Medical University
Zhejiang Hospital of Traditional Chinese Medicine
Hangzhou
Zhejiang 310006
CHINA

E-mail: yajinglin64@gmail.com
chenyaqin1121234@outlook.com

https://orcid.org/0009-0008-6716-3919